5th International Conference
on High Performance Marine Vehicles,
8-10 November, 2006, Australia

A Computing Method for the Flow Analysis around a Prismatic Planing-Hull

Hajime Kihara, National Defense Academy of Japan, Yokosuka/Japan, hkihara@nda.ac.jp

Abstract

This paper describes the computing method for the nonlinear free surface flow including a splash caused by a high-speed vessel. The 2D+T method, which is a kind of slender body theory, is employed in the present numerical studies. The idea of the domain decomposition by the boundary element method is introduced to describe the split-off of the jet domain, which enables long time simulation in spite of the spray or the splash ejection. Although the proposed numerical approach is based on the potential theory, it is a powerful tool for the nonlinear interaction between the fluid and the hull moving at very high-speed.

1. Introduction

The studies on high-speed vessels have very long history. Today the theoretical studies are still challenging issues and the investigation on their hydrodynamic properties is continued. The higher a vessel runs, the more the spray resistance increases, which is an inevitable fact. When the technology of the numerical analysis and the elucidation of complex fluid phenomena make progress more, a new tool to discuss the hull design from such a viewpoint may appear in the near future.

The numerical simulation of the flow including splashes around the planing hull is studied in the paper. Our approach is the time-domain solution method where the moving boundary of the free surface is followed by solving the boundary value problem (BVP) every time step. This is called the mixed-Eulerian-Lagrangian (MEL) approach, where the use of the boundary element method (BEM) is employed. The 2D+T method is coupled with the MEL for the computation of the wave field of a planing hull. In the case of a prismatic hull, the problem is equivalent to the water entry problem of a wedge, because of uniform section form. The problem of a two-dimensional section with knuckles is analyzed by Arai et al. (1994), Zhao et al. (1996) and Song et al. (1996). Recently the hydrodynamic properties of prismatic planing hulls are investigated using the 2D+T approach by Battistin et al. (2003). The MPS method, which is a kind of particle method, is applied to the flow analysis by Akimoto et al. (2004).

The present paper focuses on the numerical model of the spray or the splash due to a planing hull. For realistic flow simulation, gravity effect is also taken into account. The computing method developed by the BEM-based 2D+T approach enables the global flow simulation around a planing hull. Especially, computational techniques for artificial liquid separation are introduced based on the idea of the domain decomposition. Since this is originally developed for realizing long time simulation, the breakup of the jet flow cannot be predicted theoretically. However, it is interesting that the artificial liquid separation exhibits partly reasonable behavior compared with actual phenomena. We try to track the separated fragmenting fluid computationally, though rational results are not obtained yet. Additionally, hydrodynamic properties could be also investigated using the present method.

2. Formulation of the problem

We consider the problem of the steadily planing hull with a trim angle τ and an advanced speed U. The deadrise angle of the wedge section is defined as β. Assuming the fluid is inviscid and incompressible and the flow is irrotational, the steady wave-making problem of the planing hull is described by using the velocity potential ϕ. According to the conventional formulation by using the coordinate system (X, Y, Z) moving with a hull in constant speed U to the positive direction in the X axis, the velocity potential are governed by the following equations:

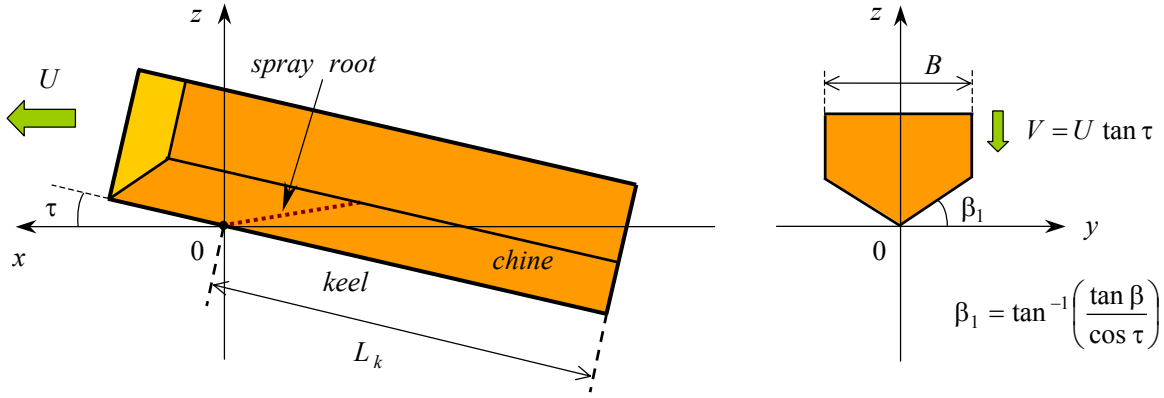

Figure 1: Definition of coordinate system

$$\frac{\partial^2\phi}{\partial X^2}+\frac{\partial^2\phi}{\partial Y^2}+\frac{\partial^2\phi}{\partial Z^2}=0 \quad \text{in} \quad \text{fluid}$$

$$-U\frac{\partial\phi}{\partial X}+\frac{1}{2}\left\{\left(\frac{\partial\phi}{\partial X}\right)^2+\left(\frac{\partial\phi}{\partial Y}\right)^2+\left(\frac{\partial\phi}{\partial Z}\right)^2\right\}+g\,\zeta=0 \quad \text{on} \quad \text{free surface}$$

$$-U\frac{\partial\zeta}{\partial X}+\frac{\partial\phi}{\partial X}\frac{\partial\zeta}{\partial X}+\frac{\partial\phi}{\partial Y}\frac{\partial\zeta}{\partial Y}-\frac{\partial\phi}{\partial Z}=0 \quad \text{on} \quad \text{free surface}$$

$$\frac{\partial\phi}{\partial n}=U\,n_X=U\sin\tau\cos\beta \quad \text{on} \quad \text{hull bottom surface}$$

where n_X is the X directional component of the normal vector on the hull surface, and g and ζ are the acceleration of gravity and the displacement of the free surface, respectively. Applying the slender body approximation, the BVP defined above can be expressed by simpler formulations (Maruo et al. 1996). The derivatives in the longitudinal direction are of lower order than those in the transverse direction. This means:

$$\frac{\partial}{\partial X} << \frac{\partial}{\partial Y}, \frac{\partial}{\partial Z}$$

Moreover, in dealing with the steady wave-making problem by the earth fixed coordinate system (x, y, z), the spacial derivative in the X direction can be transformed by the time derivative as follows:

$$\frac{\partial}{\partial t}=-U\frac{\partial}{\partial X}$$

where the space derivative in the transverse directions has no change in the transformation of the coordinate system.

Finally we obtain the two-dimensional problem to be solved in the yz plane, which is defined by using the earth fixed coordinate system. Then the velocity potential is governed by the following equations:

$$\frac{\partial^2 \phi}{\partial y^2} + \frac{\partial^2 \phi}{\partial z^2} = 0 \quad \text{in} \quad \text{fluid}$$

$$\frac{\partial \phi}{\partial t} + \frac{1}{2}\left\{ \left(\frac{\partial \phi}{\partial y} \right)^2 + \left(\frac{\partial \phi}{\partial z} \right)^2 \right\} + g\,\zeta = 0 \quad \text{on} \quad \text{free surface}$$

$$\frac{\partial \zeta}{\partial t} + \frac{\partial \phi}{\partial y}\frac{\partial \zeta}{\partial y} - \frac{\partial \phi}{\partial z} = 0 \quad \text{on} \quad \text{free surface}$$

$$\frac{\partial \phi}{\partial n} = V \cos\beta \quad \text{on} \quad \text{hull bottom surface}$$

where V corresponds to the drop speed of the wedge section on the yz plane. The hull pierces a control plane fixed in space at $x = 0$ as shown in Figure 1. Then a problem with instantaneous boundary conditions can be sequentially solved in the control plane. This is equivalent to the two-dimensional water entry problem of the wedge in the case of a prismatic hull. Thus the wave field around the hull is formulated as the initial boundary value problem (IBVP). The angle β_1 on the control plane is slightly larger than the deadrise angle β. The keel wetted length L_k is defined as the keel length below the undisturbed water surface. Although the change of wetted length is important from a viewpoint of hydrodynamic property, the attitude change of the hull in running is not considered in the present studies.

3. Numerical models

3.1. Time domain computation using BEM

The MEL approach is employed to obtain the solution of the IBVP. Numerical procedures are described by Kihara (2004), and the same manners can be used here. That is, the BVP is solved using the BEM by considering the necessary boundaries besides the free surface and the hull surface. The free surface is updated by integrating the free surface condition every time step. The outlines of the present approach are as follows:

- Introducing linear isoparametric elements for the discretization of boundaries
- Placing the double nodes on the corner point, such as an intersection of the free surface with the hull surface
- Excluding the bottom boundary from the computation due to introducing mirror image
- Performing integration analytically for every element
- Using 4th order Runnge-Kutta scheme for the time integration
- Controlling nodal density on the boundary for keeping high resolution and saving time expense in the computation

The Lagrangian form is convenient for the computation because we continue to follow the fluid particles on the free surface. We can rewrite the two free surface conditions as follows:

$$\frac{D\phi}{Dt} = \frac{1}{2}\left\{ \left(\frac{\partial \phi}{\partial y} \right)^2 + \left(\frac{\partial \phi}{\partial z} \right)^2 \right\} - g\,\zeta \qquad \text{on free surface}$$

$$\frac{D\boldsymbol{x}}{Dt} = \nabla\phi \qquad \text{on free surface}$$

where the operator D/Dt is the material derivative, and the position vector of arbitrary point on the control plane is expressed by $\boldsymbol{x} = (y, z)$. The above equations are used to obtain the velocity potential value and the position of the free surface at a next time step.

The pressure on the wetted surface of the hull can be computed by the following equation:

$$\frac{p}{\rho} = -\frac{\partial \phi}{\partial t} - \frac{1}{2}\left\{\left(\frac{\partial \phi}{\partial y}\right)^2 + \left(\frac{\partial \phi}{\partial z}\right)^2\right\} - g z$$

where ρ denotes the density of the fluid. For the pressure computation we need the $\partial\phi/\partial t$ value. Although it can be computed using the backward difference scheme, we adopt the solution procedure based on the integral equation approach for higher accuracy. It means that we solve the following boundary problem as for $\partial\phi/\partial t \equiv \phi_t$:

$$\frac{\partial^2 \phi_t}{\partial y^2} + \frac{\partial^2 \phi_t}{\partial z^2} = 0 \quad \text{in} \quad \text{fluid}$$

$$\phi_t = -\frac{1}{2}\left\{\left(\frac{\partial \phi}{\partial y}\right)^2 + \left(\frac{\partial \phi}{\partial z}\right)^2\right\} - g\zeta \quad \text{on} \quad \text{free surface}$$

$$\frac{\partial \phi_t}{\partial n} = \frac{\partial \phi}{\partial n}\frac{\partial^2 \phi}{\partial s^2} - \frac{\partial \phi}{\partial s}\frac{\partial}{\partial s}\frac{\partial \phi}{\partial n} \quad \text{on} \quad \text{hull bottom surface}$$

where the operator $\partial/\partial s$ is the tangential derivative along the boundary. We can make use of the common matrix about the boundary integral equation in two BVPs, so the computational load doesn't increased so much.

3.2 Domain decomposition for jet flow

The impulsive motion of a body induces very large acceleration near the intersection. Then the jet flow arises, so that the fluid runs up along the body surface quickly. We can trace the motion of the jet flow to some extent, but computational efforts will be added more and more because of increase of a computational domain. Consequently, such a situation leads to the numerical instabilities bringing the small negative pressure or the contact of the boundary due to thin fluid layer causing the computational break. From the above-mentioned considerations, we introduced the cut-off model to be applied only to the tip of jet flow and investigated the fluid ejection due to the gravity effect by author (Kihara 2004). According to the results, the smaller the deadrise angle is, the longer time is needed for the fluid ejection due to the gravity effect to start. It means that we need not to take into account the plunging-breaker-like splash formation in the water impact problem. Additionally it is doubtful whether the jet flow actually forms a continuous fluid domain or not, and the pressure acting on the body in the jet domain except for the spray root is equal to atmospheric one. Therefore, from a viewpoint of practical computation, we reach the assumption that the jet flow does not always have to form a single domain and part of the jet flow should break up into small fluid fragments. We'd like to emphasize that our treatment of the jet flow results from the investigation of such issues, though some computational treatments have been already introduced in other methods by using BEM or FDM.

Now we consider how to describe the split-off of the jet domain in the computation. It can be realized based on the idea of the domain decomposition by BEM. The shape of the jet domain and the dynamic pressure component on the wedge are shown in Figure 2, where the points on the boundary are nodes actually used in the computation. The computational domain is decomposed into two parts by the interface boundary AB , that is, the jet domain as sub-domain and the rest fluid domain as main-domain. Since the BVPs of both domains are coupled to solve, the solutions are rationally obtained on the whole boundary. The interface boundary can be discretized with some elements though only an element is used in Figure 2. In addition, it is not always perpendicular to the body surface, and its location can be chosen freely to some extent. When it is too close to the tip of the jet flow, we have to

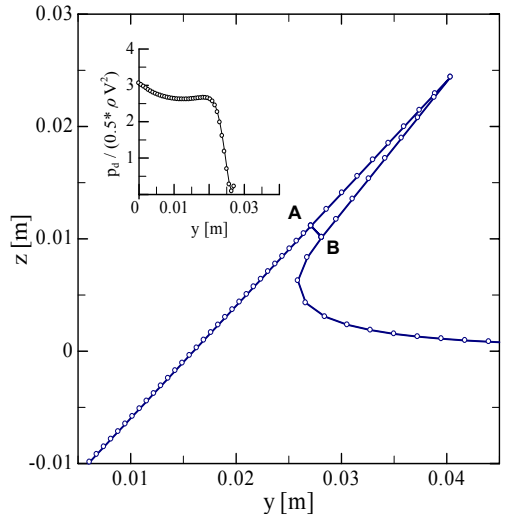

Figure 2: Domain decomposition of jet domain

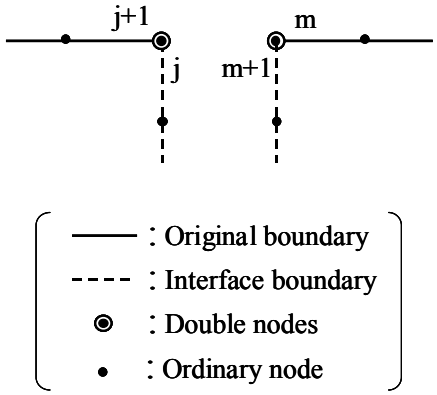

Figure 3: Nodal arrangement for matching domains

deal with much jet domain for solving the main-domain. Computational efforts such as shape description of thin jet layer and increases of nodes come out, nevertheless they may bring fruitless results. On the other hand, when it is too close to the spray root, the significant pressure value may be failed to capture, for the pressure computation may be influenced by removing the fluid providing large pressure, particularly in the case of small deadrise angle. It is not easy to suppress the small instability in pressure computation at an end-point perfectly even with the successful domain decomposition, as shown in Figure 2. This is somewhere similar to the pressure computation in the jet domain without special treatments. However, the split-off of the jet domain brings the advantage of reducing the computational trouble that the jet domain causes. We execute the domain decomposition every time the jet flow is developed too much and the criterion for the jet flow's length is violated. Then the decomposed sub-domain is regarded as fluid ejection into air like the spray or the splash.

For executing this domain decomposition exactly, the adequate boundary condition is necessary to be imposed on the interface boundary. As shown in Figure 3, introducing the double nodes on the corner (corresponding to A or B), we can make both domains matched on the interface boundary accurately. Generally there is concern about less computational accuracy in using the domain decomposition by BEM, than the computational accuracy in the single domain. However, the constant elements have been introduced in such most cases. That is, the reason is mainly the matching conditions cannot be satisfied in using the constant elements to the fullest extent, especially to the flux on the corner. Notably the use of linear elements also brings such a merit. Matching conditions at a junction are described as follows:

(i) On the boundary with Neumann condition

$$(\phi)_{j+1} = (\phi)_j \qquad \text{at} \quad \text{node } j+1$$

$$(\phi)_m = (\phi)_{m+1} \qquad \text{at} \quad \text{node } m$$

(ii) On the boundary with Dirichlet condition

$$(\phi)_{j+1} = (\phi)_j \qquad \text{at} \quad \text{node } j+1$$

$$\left(\frac{\partial \phi}{\partial n}\right)_m = \left(\frac{\partial \phi}{\partial n}\right)_{j+1} \qquad \text{at} \quad \text{node } m$$

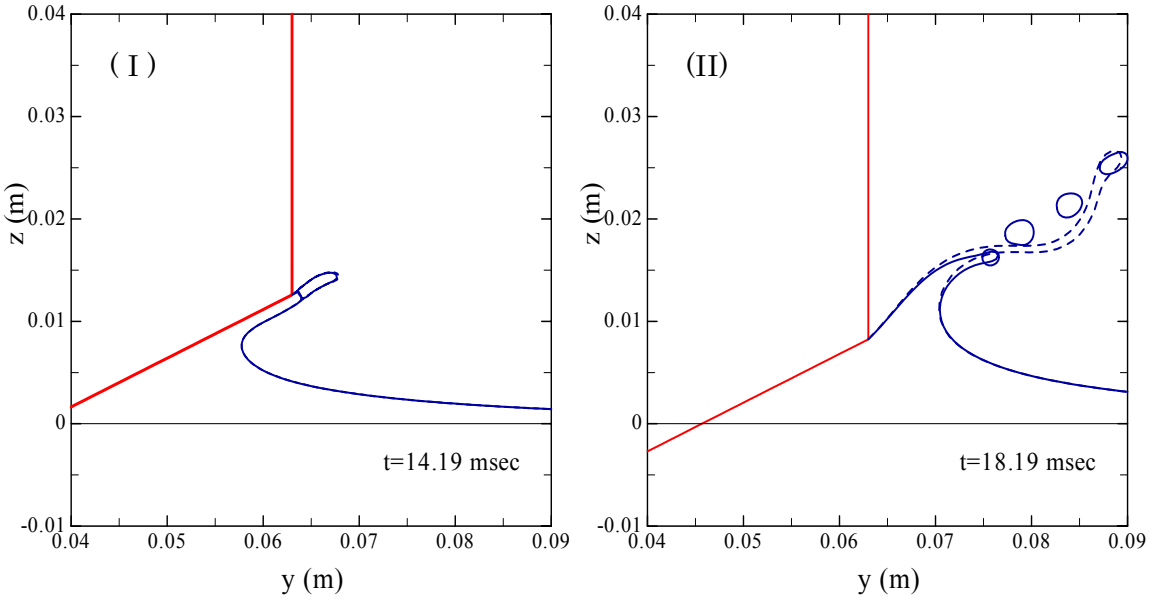

Figure 4: Simulation of splash ejected from a knuckle (Solid/dotted lines are computational results with/without executing the fluid split-off. $\beta = 25\,\mathrm{deg}$, V=1.08 m/s, B=0.126m)

(iii) On the interface boundary

$$(\phi)_j = (\phi)_{m+1} \qquad \text{at} \quad \text{node } j$$

$$\left(\frac{\partial \phi}{\partial n}\right)_j = \left(\frac{\partial \phi}{\partial n}\right)_{m+1} \qquad \text{at} \quad \text{node } m+1$$

where the index symbols such as j and m correspond to the node number in Figure 3. Although the condition that two potential values are equal is basically imposed on the double nodes, we might have to exchange the potential condition for another condition that two flux values are equal. This is a key point particularly in matching on the Dirichlet boundary. In addition, there is an alternative way to the domain decomposition for the present purpose. It's the practical procedure by the interpolation, where all values on the inner boundary for splitting a domain into two are predicted using computational results. This is a more simple procedure and brings satisfactory results practically, which was called the cut-off model and already made sure of by author (Kihara 2004). In principle, it works reasonably in the simple flow like uniform flow. The domain decomposition by the coupling computation for two domains is introduced only at the first time step, while the practical approach based on the interpolation is adopted in computing afterward.

3.3. Description of generated splash

In the case of a prismatic hull with flat bottom the hard-chine becomes separation point clearly. Since the motion of fluid particles are computed by the Lagrangian manners, that is, by using the tangential and normal components of its velocity, the flow leaves tangentially at the knuckle in viewing from the hull. Therefore, the additionally special condition like a Kutta condition is not necessary for the fluid ejection from a knuckle. However, the type of the boundary condition has to be changed before and after the ejection for sequential computation. Then the pressure condition is imposed through the dynamic free surface condition automatically. These boundary conditions are written as follows:

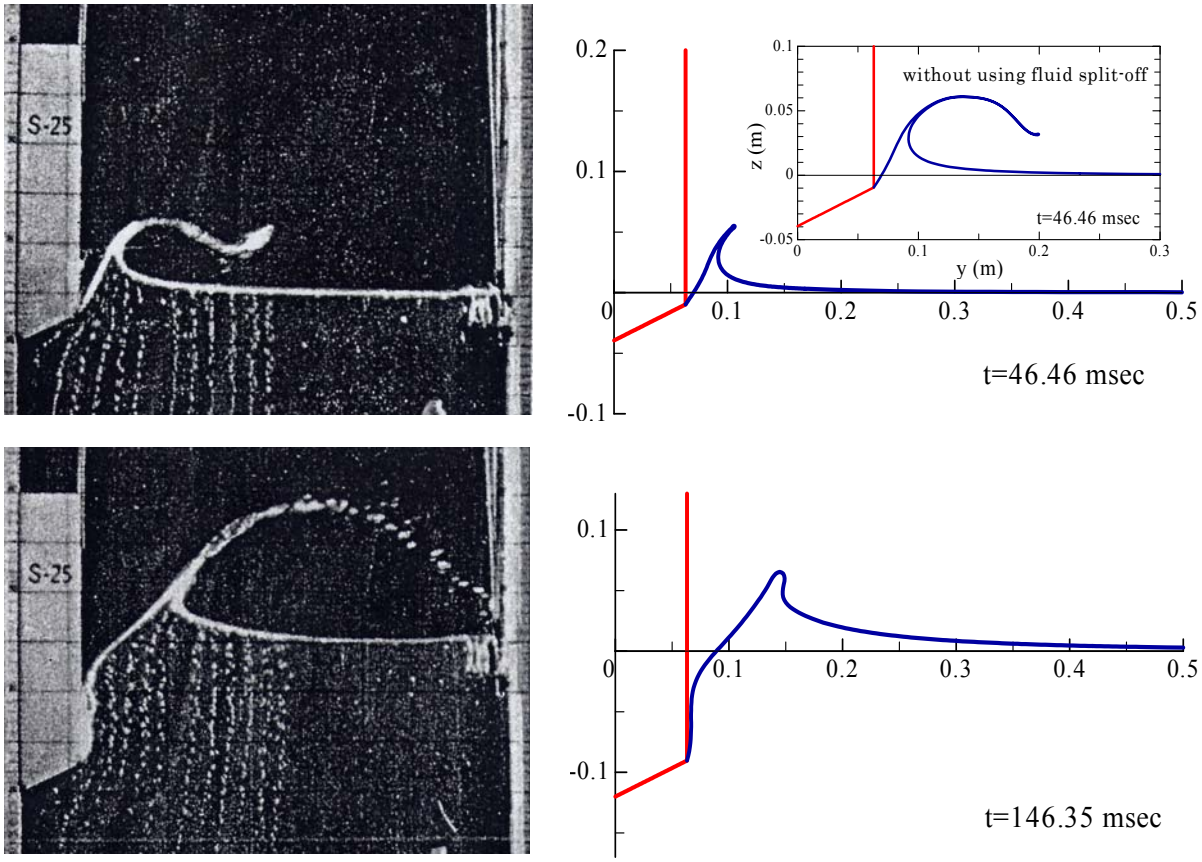

Figure 5: Comparisons between experimental results by Kikuhara (1960) and computational ones ($\beta = 25\,\mathrm{deg}$, V=0.80 m/s, B=0.126m)

$$\frac{\partial \phi}{\partial n} = \frac{\overline{\partial \phi}}{\partial n} \quad \text{(Neumann condition) as hull bottom surface in } t < t_{\text{eject}}$$

$$\phi = \overline{\phi} \quad \text{(Dirichlet condition) as free surface in } t \geq t_{\text{eject}}$$

where the symbol $\overline{\ }$ is known quantities, and t_{eject} is the time the fluid is ejected from a knuckle.

We can continue to track the fluid motion even after the fluid ejection, until the fluid boundaries overlap each other somewhere. Applying our technique of the domain decomposition as described in the section 3.2, we can avoid the difficulty by overlapping. These applications are shown in Figure 4. The case (I) is the moment for the splash to be split at the knuckle. As the jet flow develops with time to form a long and thin domain, there comes out a locally shrunk area in spite of such split-off at the knuckle. The case (II) corresponds to the moment for the fourth split-off to be executed before such a shrunk area is formed. So four droplets are described in the figure of case (II), where the farthest droplet from the body is one by the split-off in case (I). Thus we can simulate the behavior of split fluid as flying droplets. Assuming that the whole domain of split fluid is filled with the perfect fluid and the flow is irrotational, this problem can be formulated as follows:

$$\frac{\partial^2 \phi}{\partial y^2} + \frac{\partial^2 \phi}{\partial z^2} = 0 \quad \text{in} \quad \Omega_{\text{droplet}}$$

$$\frac{\partial \phi}{\partial t}+\frac{1}{2}\left\{\left(\frac{\partial \phi}{\partial y}\right)^2+\left(\frac{\partial \phi}{\partial z}\right)^2\right\}+g\,\zeta+\nu\kappa+\mu\phi=0 \quad \text{on} \quad \Gamma_{\text{droplet}}$$

$$\frac{\partial \zeta}{\partial t}+\frac{\partial \phi}{\partial y}\frac{\partial \zeta}{\partial y}-\frac{\partial \phi}{\partial z}=0 \quad \text{on} \quad \Gamma_{\text{droplet}}$$

where the symbol Ω and Γ are the fluid domain and the surrounding boundary of a droplet, respectively. Moreover, ν is a coefficient of surface tension of the fluid surface, and κ is curvature of it, which is given as $\sqrt{\left(\partial^2 y/\partial s^2\right)^2+\left(\partial^2 z/\partial s^2\right)^2}$, and μ is the artificial damping coefficient. The last term in the dynamic free surface condition is introduced to suppress the shape's motion of the droplet. It should be an important issue to decide the size of a sub-domain to be decomposed. We get through the issue by setting the criteria about both thickness and length of the jet domain. The motion of a droplet can be computed by the same procedure as the MEL approach described in section 3.1. That is, for each fluid particle that consists of the boundary of a droplet, the motion is computed by solving the above-formulated BVP every time step. Since we employing the 2D+T approach, the *x* directional velocity is supposed to be equal to an advanced speed of a planing hull in the study.

4. Numerical results

Experimental studies using planning hulls have been studied by a lot of researchers, e.g. by Savitsky (1988). Kikuhara (1960) also carried out extensive investigation of the mechanism on spray generation for the performance development of a seaplane. All computational conditions are decided assuming the comparisons with his results in the present studies.

4.1. Comparisons with experiments

We compared between experimental and computational results about the splash ejected from the knuckle, as shown in Figure 5. Two pictures on the left side are quoted from results by Kikuhara, from which we can observe the fluid domain is not continuous any more after the fluid ejection. Two figures on the right side are our computations corresponding to those. The jet flow generated on the hull bottom and the splash ejected from the knuckle are artificially decomposed in the computations. Excluding the fragmenting fluid, the present computations capture the free surface shape well. In the computational result at t=46.46 (msec), the result without using the fluid split-off is also shown. Although this result captures almost perfectly the free surface shape in the experiment, the computation breaks down due to the boundary's overlapping after a few time steps.

4.2. Feasibility studies about flying droplets

We described how to compute the flying droplets in the latter half of section 3.3, but expected results could not be obtained in the present stage. Generally it is known that the spray generated around a planning hull consists of two kinds, that is, one is the whisker spray that generates from the spray root line, and the other is the spray blister that generates from the intersection of the spray root line with the chine line. According to the observation by Latorre (1983) and Hirano et al. (1990), after both spray ejection, the former spreads ahead of the latter, and the former flow volume is more than the latter's. On the other hand, the computed droplets, corresponding to the whisker spray, don't spread off the hull into transverse direction as much as expected. The mean velocity in the horizontal or *y* direction is damped very quickly in the computation, though the numerical damping is artificially made in using the evolution equation of the velocity potential in the present scheme We estimate the mean velocity of a droplet as a mean value of velocity about all nodes on the boundary in the study.

Let us consider from another viewpoint. Assuming that the drag proportional to the square of velocity acts on the splash flying in the air, the motion equation of the splash filled with the fluid of the density

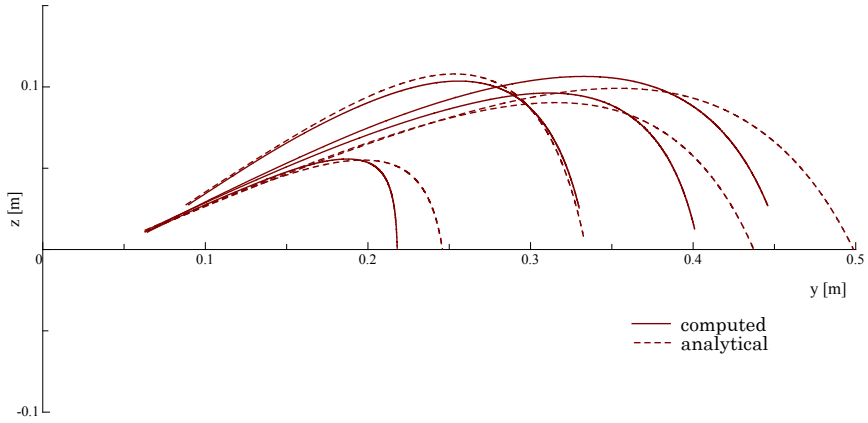

Figure 6: Projectile paths of droplets ejected from the chine (ρ_a =1.205 kg/m^3 , ρ_w =998.2 kg/m^3)

ρ_w , having mass m , is expressed as follows:

$$m\dot{\boldsymbol{v}} = -\frac{1}{2} C_D \rho_a \,|\boldsymbol{v}|\boldsymbol{v}\; d + \boldsymbol{K}$$

where C_D is the drag coefficient of a circular cylinder, and d is its diameter. The conservative force is expressed by $\boldsymbol{K} = (0, -mg)$ on $yz-$plane, and ρ_a denotes the density of the air. Projectile paths of the droplets corresponding to the spray blister are shown in Figure 6. The larger a droplet is, the farther it flies, because the Reynolds number becomes small and the drag decreases. The dotted lines in Figure 6 are results by solving the motion equation and the solid lines are ones by solving the BVP by the BEM. In these computations using the BEM, it was not easy to keep the droplet motion captured without collapsing a tiny domain though the computation was carried out to conserve the fluid volume. In some cases, we could not but give up continuing the chase. Since we employed the smoothing positively to overcome such situations, this is considered to be another factor for causing large numerical damping. However, it is interesting that those numerical damping is roughly modelled by the drag proportional to the square of velocity of the droplet. For the numerical modelling of droplets, more detailed investigation should be added forward.

4.3. Global simulation around a planing hull

Perspective views of the flow around the planning hull are shown in Figure 7. Three results on the left side are by the idea how the splash is described as continuous fluid long as possible. If more computational nodes are used for the numerical description of the splash, the broader sheet area of the splash can be simulated, but we didn't do so for the robust computation without the breakdown. The other results on the right side are by the idea how the splash is described as fragmenting fluid. Both approaches are valid for the nonlinear flow simulation around a planning hull, and the latter approach is more practical in terms of avoiding the computational drawbacks due to the boundary's overlapping.

5. Concluding remarks

The computing method for the flow analysis around a prismatic planning hull could be developed in the present study. Constructed by the BEM-based 2D+T approach, it enables the numerical model of the spray generation. Additionally, the computational treatment was theoretically made clear in our introducing the idea of the domain decomposition for the splash. Although the computational procedures of projectile droplets must be more investigated, it was recognized that the present method was robust even to the nonlinear phenomena in the fluid motion.

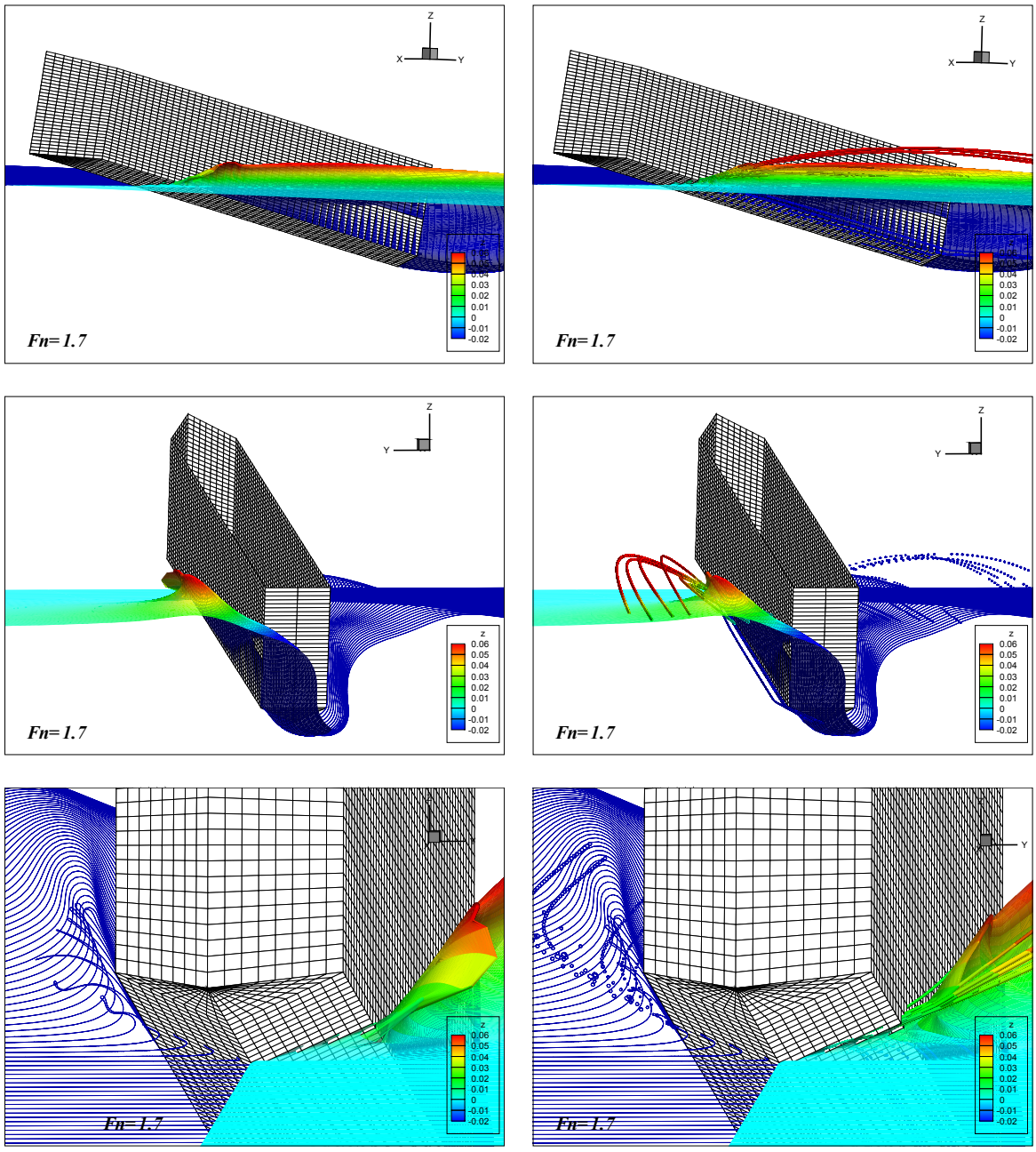

Figure 7: Computed results around the hull (L_k =1.0m, B=0.126m, τ=11.5deg, β=25deg, U=5.33m/s, FnL_k =1.7, FnB = 4.8)

References

Akimoto, H., Iida, K. and Kubo, S. (2004): "Numerical Simulation of the Flow around a Planing Wedged Cylinder by a Particle Method", *Journal of the Society of Naval Architects of Japan*, Vol.196, pp.81-89

Arai, M., Cheng, L. L. and Inoue, Y. (1994): "A Computing Method for the Analysis of Water Impact of Arbitrary Shaped Bodies", *Journal of the Society of Naval Architects of Japan*, Vol.176, pp.233-239

Battistin, D. and Iafrati, A. (2003): "A Numerical Model for Hydrodynamic of Planing Surfaces", *Proc.7th Int. Conf. Fast Sea Transportation FAST2003*, pp.33-38

Hirano, S., Inatsu, S. and Himeno, Y. (1990): "Observation of the Spray of Prismatic-Hull Models", *Journal of the Kansai Society of Naval Architects, Japan*, Vol.214, pp.65-73

Kihara, H. (2004): "Numerical Models of Water Impact", *Proc.4th Int. Conf. on High-Performance Marine Vehicles*, pp.200-214

Kikuhara, S. (1960): "A study of spray generated by seaplane hulls", *Journal of the Aero/Space Sciences*, pp.415-428

Latorre, R. (1983): "Study of Prismatic Planing Model Spray and Resistance Components", *Journal of Ship Research*, Vol.27, pp.187-196

Maruo, H. and Song, W. (1996): "Analysis of Bow Wave Breaking by the Slender Body Approximation", *Journal of the Society of Naval Architects of Japan*, Vol.175, pp.25-29

Savitsky, D. (1988): "Wake Shapes behind Planing Hull Forms", *Proc. Int. High-Performance Vehicle Conference*, pp.1-15

Song, W., Arai, M. and Maruo, H. (1996): "Nonlinear Free Surface Flow, Numerical Approach to Water Entry of Wedges and Experimental Appraisal", 19th ICTAM

Zhao, R., Faltinsen, O. and Aarsnes, J. (1996): "Water Entry of Arbitrary Two-Dimensional Section with and Without Flow Separation", *Proc. 21th Symp. on Naval Hydrodynamics*, pp.408-423